Rotational assignment using phase relationships in optical–optical double resonance: The BaI $C^2\Pi$–$X^2\Sigma^+$ system

M. A. Johnson, and Richard N. Zare

Citation: The Journal of Chemical Physics **82**, 4449 (1985); doi: 10.1063/1.448748
View online: https://doi.org/10.1063/1.448748
View Table of Contents: http://aip.scitation.org/toc/jcp/82/10
Published by the American Institute of Physics

Rotational assignment using phase relationships in optical–optical double resonance: The BaI $C\ ^2\Pi$–$X\ ^2\Sigma^+$ system

Mark A. Johnson[a] and Richard N. Zare
Department of Chemistry, Stanford University, Stanford, California 94305

(Received 20 August 1984; accepted 2 November 1984)

We describe an optical–optical double resonance scheme in which a lower vibration-rotation level is labeled. One laser is fixed in frequency and probes the population of the labeled level via the resulting laser-induced fluorescence; a second laser is scanned in frequency through the same vibronic band excited by the probe. A double resonance signal results when the population in the labeled level is either increased or decreased by the action of the second laser. The positions and phase pattern of the double resonance spectrum reveal the J numbering of the labeled level and permit a good approximation to be made for the upper and lower state rotational constants. This information allows the J value of the labeled level to be systematically changed, permitting the spectrum to be unraveled. This technique is proven by applying it to the highly congested C–X spectrum of the BaI molecule, for which no rotational information was previously available for any of its states.

I. INTRODUCTION

Laser methods in spectroscopy are now well established as a means to unravel the optical spectra of a large class of diatomic and small polyatomic molecules.[1] Most widely used among these are the methods for obtaining Doppler-free spectra through the use of saturation spectroscopy.[2] Often very complex spectra can be assigned when the congestion due to overlapping lines is eliminated. However, there is a class of molecules which are still a problem even in the absence of heterogeneous broadening either because of extensive perturbations, such as the CO_2^+ 2900 Å band system[3] and the visible spectra of NO_2[4] and FeO,[5] or because of high line density as was the case in CS_2[6] and in the present case, BaI.[7] In these cases, the problem of assignment arises because patterns among the lines cannot be recognized and traditional trial and error assignment methods based on combination differences fail since there is no way to establish the uniqueness of the assignment. The BaI molecule is such a system, and prior to our efforts,[7] none of its electronic states had been rotationally analyzed. The difficulty in finding patterns in the rotationally resolved spectrum is illustrated by the excitation spectra shown in Fig. 1. The upper trace [Fig. 1(a)] shows the vibrational structure in one spin-orbit subband of the BaI $C\ ^2\Pi$–$X\ ^2\Sigma^+$ spectrum when BaI is formed in a thermal (1250 K) molecular beam. The middle trace [Fig. 1(b)] shows the (0, 0) band spectrum at higher resolution in which the excitation linewidth is essentially the same as the Doppler width obtained in "Broida oven" sources.[8] No isolated rotational lines are yet observed. The lower trace [Fig. 1(c)] gives the single mode dye laser excitation spectrum of an 0.5 cm^{-1} section of the (0, 0) band. Some Doppler reduction ($\Delta\nu$ = 150 MHz) has been obtained by using a collimated molecular beam BaI source. The line density in the spectrum shown in Fig. 1(c) is greater than 1000 per cm^{-1}, even though this section is still "open" compared to the regions near bandheads. With usual single mode cw dye laser spectroscopy methods, lines are determined to an absolute accuracy of ± 0.005 cm^{-1}, so that several lines lie in a given range where a combination-difference search[9] would predict the presence of one. Thus, the usual methods employed to analyze plate spectra are inadequate at the precision to which line positions are routinely measured. Moreover, even if the lines of the BaI C–X system were precisely measured through sub-Doppler techniques, assignment of the spectrum would still require a full solution to the hyperfine problem since the hyperfine splittings are *themselves* on the order of 0.005 cm^{-1}.

In a case such as BaI, where the cause for congestion is primarily due to overlap rather than perturbations, the regularities in the spectrum can be revealed by narrow band filtering of the laser-excited fluorescence. This method is often referred to as "selectively detected laser-induced fluorescence" (SDLIF)[10–12] and its effectiveness on the BaI system can be appreciated by observing the degree of simplification obtained by it in Fig. 2 (spectrum taken from Ref. 13). The upper trace [Fig. 2(a)] shows the excitation spectrum of the bandhead region of the $C\ ^2\Pi$–$X\ ^2\Sigma^+$ (1, 1) band, while the lower trace [Fig. 2(b)] is the SDLIF spectrum of the *same* region. SDLIF can be used to yield an assignment of a spectrum such as that in Fig. 2(a), but requires a modest amount of work to ensure the J numbering of the lines is unique. SDLIF was used to extend the assignments made in this work for spectroscopic analysis,[13] and has also been developed as a rotational level population diagnostic in reactive scattering experiments.[14,15]

We describe here a new type of method that yields a yet higher level of simplification as well as systematically provides the J assignments and the relative magnitudes

[a] Present address: Joint Institute for Laboratory Astrophysics, University of Colorado and National Bureau of Standards, Boulder, CO 80309.

 0021-9606/85/104449-11$02.10

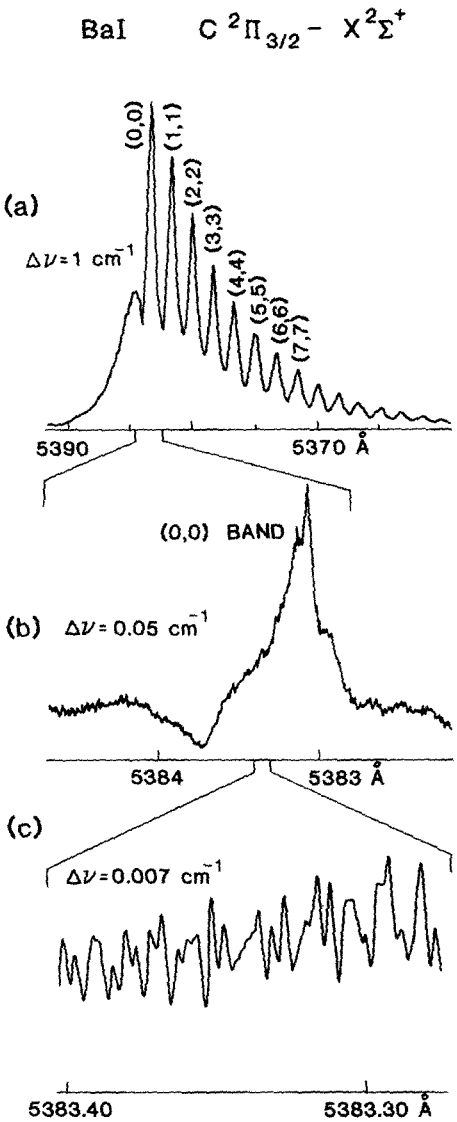

FIG. 1. Survey excitation spectra of the BaI $C\,^2\Pi_{3/2}$–$X\,^2\Sigma^+$ subband. (a) Vibrational structure of the spectrum when BaI is formed in a molecular beam source; (b) expansion of the (0, 0) band at a resolution corresponding to that obtained in traditional oven or flame sources; and (c) further expansion of the (0, 0) band taken with a single-mode laser exciting a collimated molecular beam of BaI.

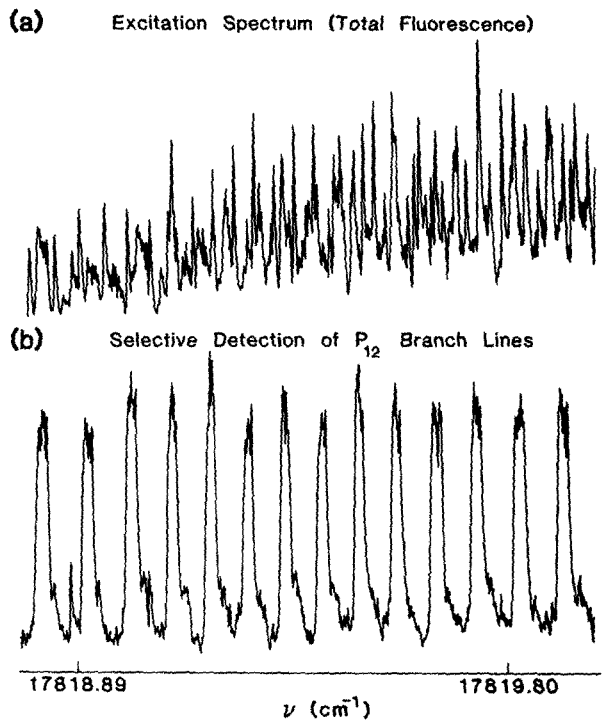

FIG. 2. Example of spectral simplification offered by selectively detected laser-induced fluorescence. (a) Single-mode scan of the overlapping (1, 1) and (2, 2) bands where all fluorescence is collected; (b) isolation of the (2, 2) P_{12} branch achieved by filtering the LIF through a monochromator.

of several spectroscopic constants in a direct and concise way. This method was described briefly in a previous communication,[7] and is an extension of the population labeling technique demonstrated by Kaminsky *et al.*[16] in 1976 and used extensively to assign the optical spectra of Cs_2,[6] NO_2,[17] CO_2^+,[18] and O_2^+.[19] Population labeling is a three-level laser spectroscopic technique and is usually used as an assignment tool which links an unknown band to one previously analyzed.[1,6,17–19] We have modified this method to handle cases such as the BaI molecule, in which no bands exist that have been previously assigned. The key to this modification lies in using the optical pumping properties inherent in an electronic system, some of whose bands have large Franck–Condon factors (in the case of BaI, the $\Delta v = 0$ sequence). This paper is concerned only with the analysis of unperturbed spectra, hence extra lines and anomolous line strengths for perturbed levels need not be considered.

II. DESCRIPTION OF THE METHOD

Figure 3 is a schematic diagram showing the levels involved in population labeling double resonance. Two lasers are used, both tuned to the rotational band structure corresponding to the transition between the electronic states to be analyzed. One laser, the *probe laser,* is fixed on the frequency of a particular rotational line and serves to monitor the population in the ground state rotational level of this transition. This lower level will be referred to as the "labeled level," denoted J_L''. The second laser, the *pump laser,* is scanned through the entire rotational

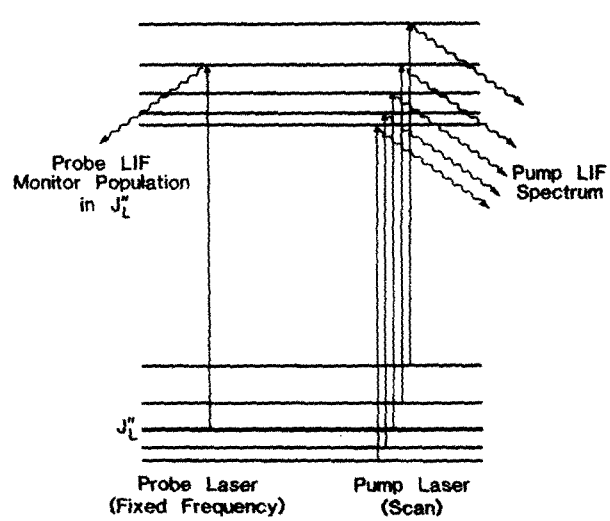

FIG. 3. Schematic diagram of population-labeling double resonance. J_L'' denotes the labeled level.

spectrum of the vibronic band in question. This laser is taken to be sufficiently powerful to pump population out of lower levels as it excites transitions.

In what follows we assume that the vibronic transition excited by the pump laser has a large Franck–Condon factor. (In the case of the BaI C–X system it is nearly unity for the $\Delta v = 0$ sequence.) This implies that population removed from a particular ground state level by the pump laser will be redistributed among neighboring rotational levels of the same vibrational state. The precise nature of this redistribution is a consequence of the dipole selection rules and band structure of the electronic transition in question; we will describe the use of this redistribution in establishing the rotational quantum number assignments.

In this experiment, the probe laser is fixed in frequency while the pump laser is scanned through the band. The fluorescence induced by the probe laser is detected and used to monitor the population in level J''_L. Since we will be primarily interested in the effects of optical pumping on timescales long compared to the lifetime of excited states, the transient population in the excited state is ignored. Whenever the pump laser coincides with a transition capable of affecting the population in J''_L, the fluorescence signal from the probe laser is altered owing to this change in population. Clearly, two kinds of transitions are possible: those that ultimately add population to J''_L, and those that subtract population from J''_L. These are distinguishable by being opposite in phase in their affect on the population in J''_L.

Since the BaI C–X system involves a $^2\Pi$–$^2\Sigma$ band, the possibilities for double resonance activity are not immediately obvious. To illustrate the method, we first describe its application to three simple cases encountered in the spectroscopy of linear molecules;

(i) $^1\Sigma$–$^1\Sigma$,

(ii) $^1\Pi$–$^1\Sigma$,

(iii) $^1\Sigma$–$^1\Pi$.

We then consider a $^2\Pi$–$^2\Sigma$ transition, and describe the application of this method to the analysis of both spin-orbit components of the C–X system of BaI. This paper is intended to describe the generation of line assignments in this system which are needed for a number of spectroscopic and reaction dynamics studies in this laboratory.[13–15] The reduction of these data to spectroscopic constants and discussion of implications regarding the electronic states of the alkaline earth halides are presented in another publication.[13]

III. DOUBLE RESONANCE PATTERNS

The general calculation of the double resonance pattern is performed in three steps. In the first step, the number and phase relationship of double resonance transitions are found using the rotational energy level diagram. In the second step, the line strengths of all the relevant transitions are calculated. Finally, in the third step, the line strengths are used to evaluate the probability of moving population into or out of the labeled level J''_L for each type of transition.

The number and phase of double resonance transitions for the case of singlet states is easily evaluated by referring to Fig. 4. In any vibronic transition, there are at most three rotational transitions (P, Q, and R) from any particular level. Thus there are at most three transitions that can remove population from the labeled level. On the other hand, other transitions terminating on the upper levels involved in these P–Q–R lines may also affect the population in J''_L. This occurs by first pumping population to the common upper level followed by radiative decay to J''_L. Since each such upper level also has at most three transitions (P, Q, R) out of it to the ground state, a total of nine transitions are capable of double resonance activity. Three of these subtract population from J''_L and are denoted by (−), while the remaining six add population to J''_L, and are denoted by (+). Fewer transitions may be observed owing to more severe selection rules in particular cases (e.g., no Q branch in $^1\Sigma$–$^1\Sigma$ transitions or missing branch members at low J).

Within a band the magnitude of the double resonance signal depends on a product of the population of the level being pumped, the line strength to the upper level J'_u, and a factor taking into account the partitioning of the fluorescence among the lower levels (J''_f). Thus for the case of adding population from J''_i to J''_L, we may write:

$$I(+) \sim \frac{N(J''_i)S(J''_i, J'_u)S(J'_u, J''_L)}{\sum_{J''_f} S(J'_u, J''_f)}, \tag{1a}$$

while for the case of subtracting population from J''_L:

$$I(-) \sim \frac{N(J''_L)S(J''_L, J'_u) \sum_{J''_f \neq J''_L} S(J'_u, J''_f)}{\sum_{J''_f} S(J'_u, J''_f)}, \tag{1b}$$

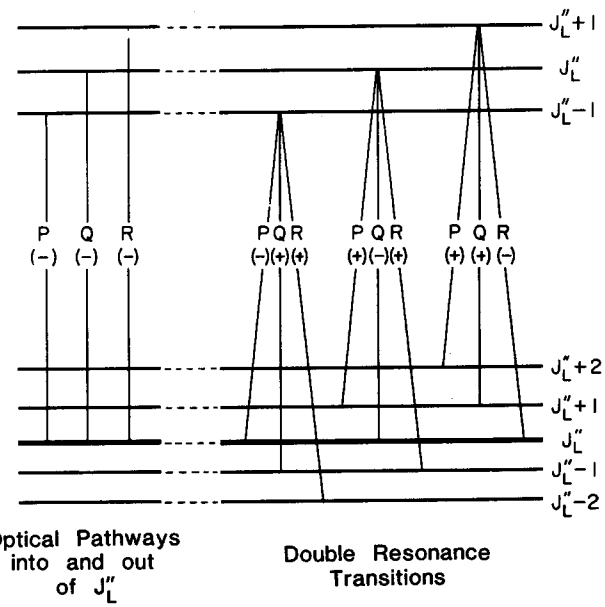

FIG. 4. Illustration of the nine possible double resonance lines for a transition between singlet electronic states. Three are (−) type and six are (+) type.

where $S(J', J'') = S(J'', J')$ denotes the rotational line strengths for electric dipole transitions between levels J' and J'', and $N(J)$ is the population in level J.

A. $^1\Sigma$–$^1\Sigma$

Since only P and R branches exist for these systems, there will be four double resonance transitions, two of which are (−) and two (+). To demonstrate the application of Eq. (1) to this case, consider the $P(J''_L)$ line which results in a (−) double resonance (DR) transition. Applying Eq. (1b), we find that the intensity of this double resonance feature is

$$I(-) \sim \frac{N(J''_L)J''_L(J''_L - 1)}{(2J''_L - 1)}. \tag{2}$$

Likewise the other three DR transitions may be calculated, and a simulated DR spectrum of the $^1\Sigma$–$^1\Sigma$ transition is presented in Fig. 5 along with a simulation of the normal LIF spectrum. While the $^1\Sigma$–$^1\Sigma$ transition is sufficiently simple that DR is usually not necessary, some of the features of Fig. 5 are noteworthy. The DR spectrum simplifies the spectroscopy because it displays all the one-photon and two-photon optically connected levels to the J''_L level [Fig. 5(c)]. This is just the information spectroscopists need when analyzing a spectrum. The assignment of quantum numbers and measurement of the rotational Hamiltonian are generated from the combination difference relations found directly in the DR spectrum.

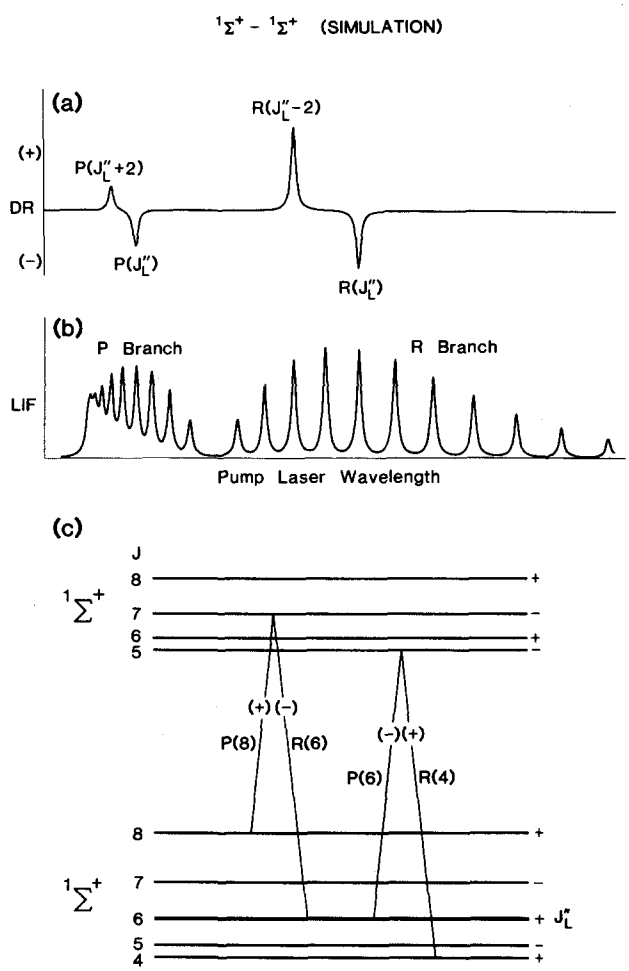

FIG. 5. Simulation of DR spectra for the $^1\Sigma^+$–$^1\Sigma^+$ transition. Conditions of the simulation: Rotational temperature 50 K, $B' = 1.1$ cm^{-1}, $B'' = 1$ cm^{-1}, and $\Delta\nu_{laser} = 0.25$ cm^{-1}, $J''_L = 6$; (a) DR spectrum from the probe laser as the pump laser is scanned; (b) LIF spectrum from the pump laser; and (c) level diagram showing the origin of DR transitions.

For example, the rotational energy expression of a $^1\Sigma$ state is given approximately by

$$E(J) = BJ(J + 1). \tag{3}$$

The (−) peaks in the DR spectrum correspond to the $P(J''_L)$ and $R(J''_L)$ lines, whose splitting (=Δ') contains upper state information exclusively. From Eq. (3),

$$\Delta'(J''_L) = 4B'(J''_L + 1/2). \tag{4}$$

A corresponding relation holds for the ground state splitting using either the $P(J''_L + 2)$ and $R(J''_L)$ or the $P(J''_L)$ and $R(J''_L - 2)$ (+)/(−) pairs, yielding $\Delta''(J''_L + 1)$ and $\Delta''(J''_L - 1)$, respectively.

Since $\Delta''(J) = 4B''(J + 1/2)$, the second difference can be found for the ground state:

$$\Delta''(J''_L + 1) - \Delta''(J''_L - 1) = 8B''. \tag{5}$$

Thus, B'' may be evaluated from *one DR scan* to sufficient accuracy to infer J''_L using either $\Delta''(J''_L - 1)$ or $\Delta''(J''_L + 1)$. Similarly, B' may then be generated using $\Delta'(J''_L)$. This illustrates that one double resonance scan can provide four J assignments to anchor the rest of the assignment of the band. Clearly, other transitions could then be used to probe different J''_L values to secure the uniqueness of the assignment.

This simple example is intended to show the strategy of the DR method in picking apart the spectrum. The DR experiment is seen to yield the electronic symmetry of the transition by the four line pattern and phase fingerprint. Analysis of this pattern reveals the branch structure of the vibronic band as well as the quantum number assignment of J''_L. In addition, first order estimates of B' and B'' are obtained. Next we turn to a more interesting case where parity doublets complicate the analysis for systems in which $\Lambda \neq 0$.

B. $^1\Pi$–$^1\Sigma^+$

Since the $^1\Pi$–$^1\Sigma$ transition is a perpendicular band, P, Q, and R transitions are allowed from J''_L. It is an interesting feature of the $^1\Pi$–$^1\Sigma$ band, however, that the levels of the Π state either radiate in P and R branches or in a single Q branch, depending on the parity of the lambda doublet [see Fig. 6(c)]. The P and R branches have two (+) and (−) DR transitions, just as for the $^1\Sigma$–$^1\Sigma$ transition, and give rise to the four-line pattern shown in Fig. 6. The $Q(J''_L)$ line is present in the LIF spectrum [Fig. 6(b)], but driving this transition does not redistribute the rotational population since all the fluorescence from the upper level occurs in just one line. Thus, significant fluorescence to other vibrational levels is required to see the (−)-type $Q(J''_L)$ transition. When the DR pattern for $J''_L + 1$ is obtained, the Λ-type doubling $\Delta_{ef}(J)$ can be determined from[9]

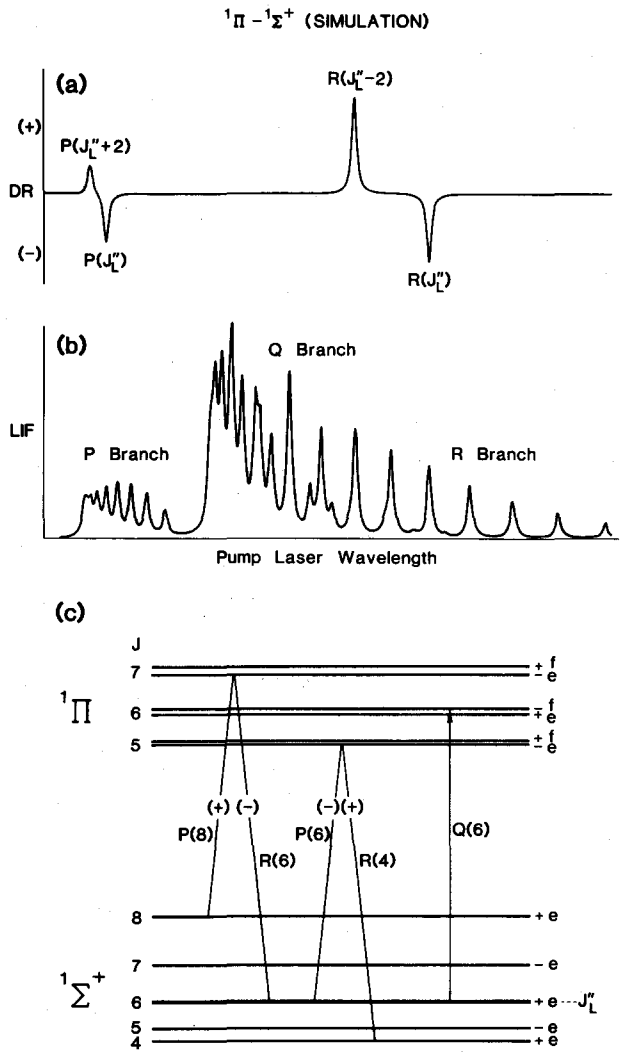

FIG. 6. Simulation of the DR spectra for the $^1\Pi$–$^1\Sigma^+$ transition. Conditions of simulation: same as for $^1\Sigma^+$–$^1\Sigma^+$ (no Λ-type doubling included). (a) DR spectrum; (b) pump LIF spectrum; and (c) level diagram showing the origin of DR transitions.

$$\Delta_{ef}(J''_L) \sim \frac{[R(J''_L) - Q(J''_L) - \{Q(J''_L + 1) - P(J''_L + 1)\}]}{2}. \tag{6}$$

Traditionally, some difficulty arises in deciding from the line spectrum alone whether a $\Delta\Lambda = 1$ band is $^1\Pi$–$^1\Sigma$ or $^1\Sigma$–$^1\Pi$. This determination requires either assigning the lowest rotational transitions in a vibronic band to find "missing" lines or dispersing the fluorescence with rotational resolution to resolve P–Q–R triplets or single Q and P–R doublet patterns. In each case, the measurements are hindered owing to small signals from sparsely populated low J levels or losses in monochromator throughput. In the next section, we demonstrate that the $^1\Pi$–$^1\Sigma$ and $^1\Sigma$–$^1\Pi$ transitions can be readily identified using their DR patterns. Since this DR method does not require dispersing the fluorescence and can be performed on thermally populated rotational levels, the identification can be made under conditions yielding a favorable signal-to-noise ratio.

C. $^1\Sigma^+$–$^1\Pi$

In the previous examples, the choice of which level is labeled as J''_L was arbitrary since, although the parity of a $^1\Sigma$ state alternates with J, the DR spectra are not dependent on this parity. With a $^1\Pi$ ground state, however, a J''_L can involve either Λ-type doublet and the DR pattern for each is quite different.

This difference between the Λ doublets is caused by the fact that one parity level supports P and R branches while the other has only a Q branch. For the purposes of this discussion, let us suppose that the $^1\Sigma$ state is a $^1\Sigma^+$ state; if it were a $^1\Sigma^-$ state the only effect is to reverse the e/f parity labels.[20] For a $^1\Sigma^+$ state, the f parity levels of the Π state are the "Q branch states."

If these f levels are the labeled levels, then there can be only one (–) type of DR line, on the $Q(J''_L)$ transition. The upper level of this Q line does, in contrast to the $^1\Pi$–$^1\Sigma^+$ case, radiate in P, Q, and R branches so that the $P(J''_L + 1)$ and $R(J''_L - 1)$ transitions give (+) DR signals. The simulated DR spectrum is shown in Fig. 7(a), with the normal LIF spectrum (simulated) in Fig. 7(c) and relevant level diagram in Fig. 7(d). Note that the Q branch contains the *only* transitions which can be used to probe f levels, the same ones which give the (–) DR features. Thus, the pattern in Fig. 7(a) reveals the Q branch of the $^1\Sigma^+$–$^1\Pi$ band.

Probing the e levels leads to quite a different situation, however, since many more DR transitions are allowed, as shown in Fig. 7(b). Alternating patterns such as those in Figs. 7(a) and 7(b) are conclusive evidence that the band is indeed $^1\Sigma^+$–$^1\Pi$ rather than $^1\Pi$–$^1\Sigma^+$. The DR pattern in Fig. 7(b) is again of the correct form to assign J''_L and extract B' and B'' values. Similarly, the Q branch may be used as in the previous example to establish the sign and magnitude of the Λ-type doubling parameter.

D. $^2\Pi$–$^2\Sigma^+$

The branch structure of a $^2\Pi$–$^2\Sigma^+$ system is the most complicated case addressed in this paper. We will treat the $^2\Sigma^+$ case, which is the symmetry of the BaI transition analyzed experimentally in Sec. IV. The treatment of the $^2\Sigma^-$ is completely analogous except for the opposite parity labels on the rotational energy levels of the $^2\Sigma^-$ state. We will only consider $^2\Pi$ states with sufficiently large spin-orbit separation so that the $^2\Pi_{1/2}$–$^2\Sigma^+$ and $^2\Pi_{3/2}$–$^2\Sigma^+$ subbands are spectrally distinct. This is a good description of the BaI molecule, for which the spin-orbit splitting[21] of ~750 cm^{-1} is large compared to the rotational constant (~0.03 cm^{-1}). Since the two spin-orbit components of such a $^2\Pi$ state behave independently in their DR behavior, we will further specialize our treatment to the analysis of one spin-orbit subband.

A subband of the $^2\Pi$–$^2\Sigma$ transition is comprised of six rotational branches, with two distinct parity species in both upper and lower states. To evaluate the number and phase relationship of the DR lines, refer to Fig. 8. Each level in this problem is optically connected to the other electronic state via P, Q, and R transitions, implying

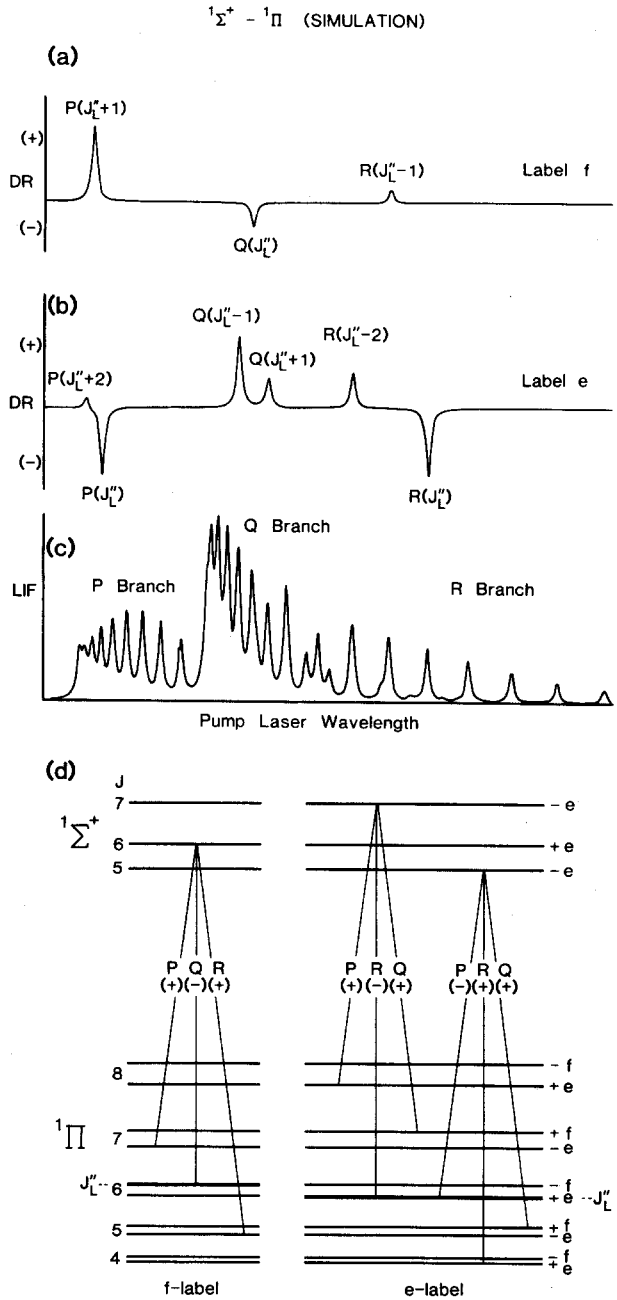

FIG. 7. Simulation of DR spectra for the $^1\Sigma^+$–$^1\Pi$ transition. Conditions of the simulation: same as for $^1\Sigma^+$–$^1\Sigma^+$ (no Λ-type doubling included). (a) DR spectrum for f-parity label; (b) DR spectrum for e-parity label; (c) LIF spectrum from pump laser (same for both DR spectra); (d) level diagrams showing the origin of DR transitions in (a) and (b).

that each DR spectrum will display nine features. As in Fig. 4, three of these will be (−) while the remaining six are (+). The particular pattern actually obtained critically depends on the magnitude of the spectroscopic constants. This is evident in Fig. 8, for example, in the $Q_2(J_L'')$ and $P_{21}(J_L''+1)$ DR lines (refer to Fig. 8). These lines are necessarily (−) and (+) types, respectively, since an f level is labeled, but the order of these lines in the spectrum depends on the sign of the spin-rotation interaction constant γ of the $^2\Sigma^+$ state. The levels in Fig. 8 are drawn for $\gamma > 0$; however a negative γ would reverse the phase of the Q_2 and P_{21} "doublet" of DR lines in the spectrum. We will show that the phase pattern obtained actually

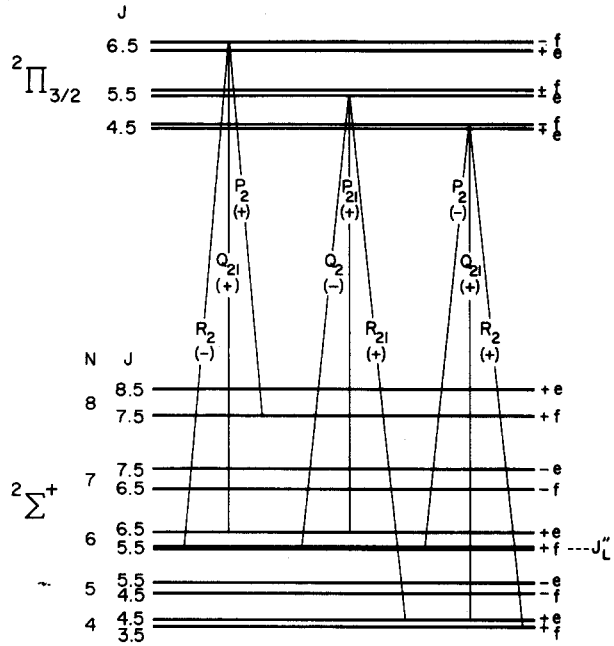

FIG. 8. Level diagram showing DR transitions for the $^2\Pi_{3/2}$–$^2\Sigma^+$ case in which the f-parity $J_L'' = 5.5$ level is labeled.

serves as a convenient method of determining the sign of the spin-rotation constant.

Fundamentally, there are four possible patterns for the DR spectrum of a $^2\Pi$–$^2\Sigma^+$ transition, and these are displayed schematically in Fig. 9. As was the case in the

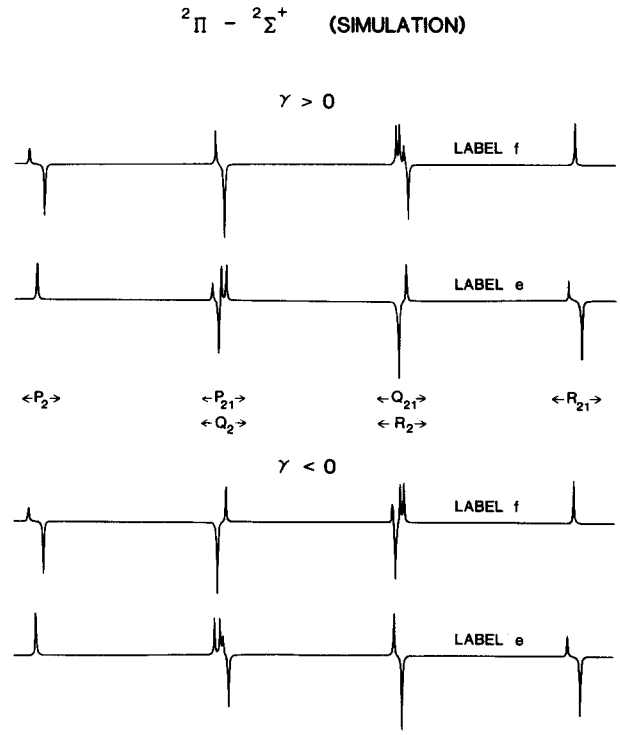

FIG. 9. Illustration of the possible DR phase patterns for the $^2\Pi$–$^2\Sigma^+$ transition (one spin-orbit subband). These particular patterns are for the BaI molecule with $J_L'' = 45.5$ using the constants obtained in Ref. 13. Note that the cluster of four lines (either in the Q_{21} and R_2, or P_{21} and Q_2 branches) has a variable pattern depending on the relative magnitudes of the branch line spacings and the spin-rotation splitting at the labeled N level of the $^2\Sigma^+$ state.

$^1\Sigma$–$^1\Pi$, two of the patterns can be accessed by changing the e/f parity component labeled as J''_L, while the other two do not exist within the same vibronic band since they apply to the other sign of γ. Thus, *one DR spectrum of the $^2\Pi$–$^2\Sigma^+$ transition immediately defines the sign of the spin-rotation constant as well as the branch structure.* The nine-line pattern facilitates the assignment of the band as a $^2\Pi$–$^2\Sigma^+$ transition, and provides direct confirmation that the band is $^2\Pi$–$^2\Sigma^+$ rather than $^2\Sigma^+$–$^2\Pi$. Moreover, the P–R structure of the DR pattern is analogous to that in Fig. 5 for the P_2 and R_2 branches, so that once again J''_L, B', and B'' are available from one DR scan.

IV. APPLICATION TO BaI

In this section, we describe a method for implementing the DR strategy discussed above to an actual system which requires the use of such a simplification to analyze its spectrum: the C–X system of the BaI molecule. This molecule serves as an excellent example of how the DR technique can be used in a practical situation.

A. Properties of the BaI C–X spectrum and description of the experiment

The BaI C–X band system shows primarily a $\Delta v = 0$ sequence at low vibrational quantum number, a common feature of the alkaline earth monohalide spectra since the transition involves nonbonding orbitals. Therefore, the visible absorption spectrum of the $v'' = 0$ level shows two bands, one at 5383 Å and the other at 5612 Å, which are separated by the spin-orbit splitting in the $C\ ^2\Pi$ state ($|\text{Å}| = \sim 750\ \text{cm}^{-1}$).[21] Due to extensive reference to a particular spin-orbit component of the $C\ ^2\Pi$ state, we will hereafter refer to the subband at 5612 Å as the C_1–X subband, and to the subband at 5383 Å as the C_2–X band. C_1 and C_2 will therefore denote the two spin-orbit components (the F_1 and F_2) of the $^2\Pi$ state, where traditionally it is assumed that $C_1 = {}^2\Pi_{1/2}$ and $C_2 = {}^2\Pi_{3/2}$.

The $C\ ^2\Pi$ lifetime has been measured[22] and found to be extremely short (17 ns), which, when combined with a Franck–Condon factor of essentially unity, implies that the oscillator strength for excitation of the C–X transition approaches that of allowed transitions in atoms. Because the origin of the C state lies well below the energy of the separated ground state atoms [Ba($^1S_0$) and $I(^2P_{3/2})$],[23] the fluorescence quantum yield is unity.

The effect of the properties mentioned above on the optical pumping DR experiment are summarized: (i) low saturation power requirements (<1 mW/cm^2), (ii) only one v'' level is affected by optical pumping, (iii) large spectral separation (230 Å) of the spin-orbit subbands in both absorption *and* fluorescence. Points (ii) and (iii) are particularly useful in the present application of DR. Point (ii) implies that if the population in one lower level (v''_L, J''_L) is depleted by optical pumping via the C–X transition, this population will be redistributed to neighboring rotational levels of the vibrational state v'' while the pump laser is on.

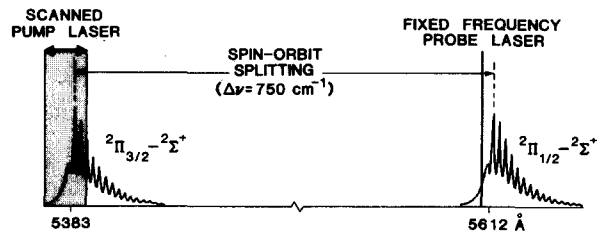

FIG. 10. Schematic diagram of the roles of the pump and probe lasers in the application of double resonance to the BaI $C\ ^2\Pi$–$X\ ^2\Sigma^+$ band.

Point (iii) is advantageous because it allows the excitation and detection scheme shown in Fig. 10. Since any transition involving J''_L will suffice to monitor the population in J''_L, it is not necessary for the probe laser to excite the same subband as is being scanned by the pump laser. *If each laser excites a different spin–orbit subband, the resulting laser excited fluorescence from each laser may be viewed independently when both lasers are on simultaneously.* Moreover, due to the large spectral separation of the fluorescence from each laser, independent detection may be accomplished with crude spectral resolution (such as long pass absorption and interference filters).

While the spectral separation of the spin-orbit subbands in the BaI C–X transition simplified the application of population labeling OODR in this molecule, intermodulated fluorescence techniques[24] could have been used to obtain the DR spectra with both lasers tuned to the same subband. In this variation, the lasers are chopped at ω_1 and ω_2, and the DR spectrum is measured by demodulating the component of the fluorescence characterized by the sum or difference frequency $\omega_1 \pm \omega_2$.

B. Experimental setup

The general arrangement of the experiment is shown in Fig. 11. BaI is formed in a molecular beam using a method described in Ref. 14. Tunable radiation (50 mW) from two single-mode cw dye lasers (Coherent 599-21 using Rhodamine 110 blue shifted by adding a pH 10 buffer solution) is obtained using 4 W all-lines Ar^+ pumps for each. The laser beams are modulated using PAR 192 choppers (400 and 100 Hz for the pump and probe lasers, respectively), and the LIF is phase sensitively detected with three PAR 124 lock-in amplifiers. The probe laser beam is focused with a 1 m lens and counterpropagated with respect to the pump beam through the molecular beam chamber, overlapping in the center of the effusive BaI beam. The background pressure in the interaction region is 5×10^{-6} Torr. The LIF from the molecular beam is imaged at $f/3$ and split into two paths with a 50% beam splitter. Each LIF beam is detected by a photomultiplier after passing through an appropriate filter to isolate one spin-orbit subband of the C–X system. The pump laser LIF spectrum is stored simultaneously with the DR spectrum in a Nicolet 1170 dual channel signal averager.

As an example of a typical experiment, laser 1 in Fig. 11 is fixed in frequency on a rotational transition of

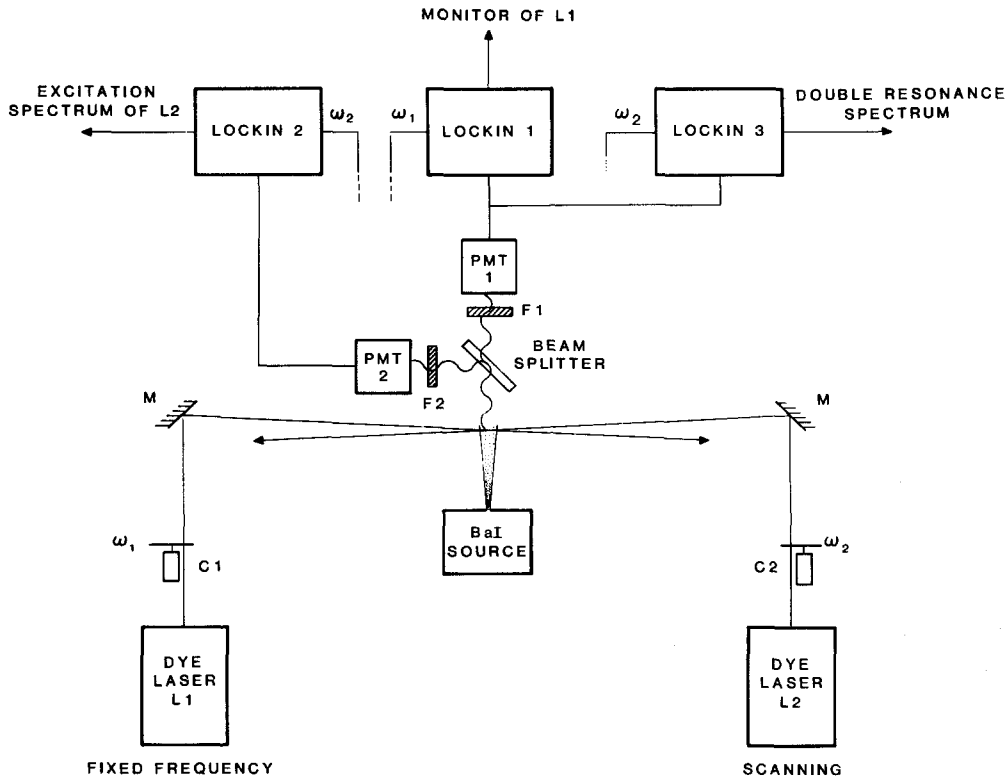

FIG. 11. Block diagram of the experiment. L = cw single-mode dye laser, C = chopper, F = filter, PMT = photomultiplier tube, M = mirror, and ω = chopping frequency.

the C_1–X system at 5612 Å and chopped at 100 Hz. Filter 1 isolates the 5612 Å fluorescence and photomultiplier 1 detects this fluorescence. The output from PMT 1 is then fed into lock-in amplifiers 1 and 3. Lock-in 1 is referenced to 100 Hz and its output is proportional to the LIF from the probe laser. The probe fluorescence is also input into lock-in 3, which is referenced to 400 Hz, the chopping frequency of the pump laser, and its output is the double-resonance signal. Similarly, the fluorescence from laser 2 is input to lock-in 2, where, in this case, the pump laser LIF spectrum is recovered.

C. Double resonance spectra of the BaI C–X (0, 0) band

Figure 12 presents a typical double resonance spectrum of the BaI C–X (0, 0) band. The upper trace is the double resonance spectrum obtained by labeling the f-parity J''_L = 9.5 level with the probe laser on the $Q_{12}(9.5)$ transition of the $C\ ^2\Pi_{1/2}$–$^2\Sigma^+$ subband near 5612 Å. The lower trace is the excitation spectrum of the $C\ ^2\Pi_{3/2}$–$X\ ^2\Sigma^+$ around 5283 Å scanned by the pump laser. The simplicity gained by the DR experiment is self-evident.

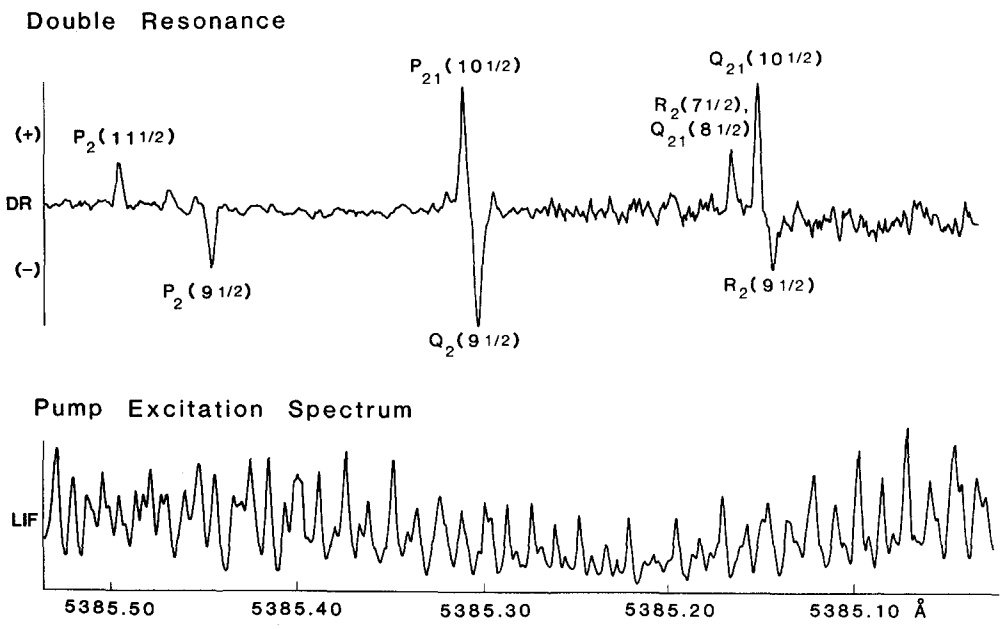

FIG. 12. DR spectrum obtained for the BaI $C\ ^2\Pi_{3/2}$–$X\ ^2\Sigma^+$ (0, 0) band. The labeled level is the f-parity J''_L = 9.5 level. (a) DR spectrum obtained from labeling the $C\ ^2\Pi_{1/2}$–$X\ ^2\Sigma^+$ subband with the $Q_{12}(9.5)$ transition; (b) LIF of the pump laser scan through the $C\ ^2\Pi_{3/2}$–$X\ ^2\Sigma^+$ subband.

The DR spectrum shows three (−) features and four (+) features. The $R_2(7.5)$ and $Q_{21}(8.5)$ (+) lines are blended and appear as one line while the remaining (+) line exists but is outside the region scanned in Fig. 12. Comparison of the phase pattern in Fig. 12 with those in Fig. 9 immediately shows that the sign of the spin-rotation constant in the $X\ ^2\Sigma^+$ state is positive and that J''_L is of f parity. We remark that the intensity pattern in the DR spectra for the BaI molecule are only approximately accounted for by the expression in Eq. (1). This is due to the hyperfine components labeled within J''_L due to the hyperfine structure of the pump transitions. Nonetheless, Eq. (1) does correctly predict the observed DR spectra to within a factor of 2 variations in the intensity pattern. Note that the DR pattern alone does not give direct information about the branch to which the labeling $C\ ^2\Pi_{1/2}$–$X\ ^2\Sigma^+$ probe transition belongs, but only the parity of the ground state probe level.

Because of the overlapping of the R_2 and Q_{21} lines in the spectrum shown in Fig. 12, it is difficult to measure the lines with sufficient accuracy to use the second difference method discussed previously [see Eq. (5)] to generate B''. Since the $P_2(J''_L)$, $R_2(J''_L)$ and $Q_2(J''_L)$ lines are available in the DR spectrum, the value of J''_L may still be evaluated as follows. From Eq. (3), the splitting between the P and Q lines $[\Delta_{PQ}(J''_L)]$ and the R and Q lines $[\Delta_{RQ}(J''_L)]$ is related to B':

$$\Delta_{RQ}(J''_L) - \Delta_{PQ}(J''_L) = 2B'.$$

This difference uses clean lines in the DR spectrum and analysis of this spectrum yields a J''_L value of 9.3 and a B' value of 0.0273 cm^{-1}. A more complete analysis[13] of many DR spectra for many J''_L levels confirms the assignment of J''_L as 9.5, and refines the measurement of B' to 0.026 727 cm^{-1}. Constants obtained from the DR scan in Fig. 12 are compared with those from a global fit to over 500 lines[13] in the BaI C–X in Table I, where it is seen that the DR spectrum gives B values good to 2% and the spin-rotation constant good to 10%. Thus, the essential features of the spectrum are obtained with just one DR scan!

It is worth mentioning that even without pausing to calculate J''_L from second differences, the DR spectra can be used to step J''_L in a known fashion. If the probe transition is changed, it is generally not known in the first iteration what J''_L level is now labeled. The phase pattern will reveal immediately, however, whether J''_L is an e or f level using the patterns in Fig. 9. This use of

TABLE I. Comparison of rotational constants for least-squares fit (>500 lines) and one DR scan (cm^{-1}).

Constant	Electronic state	One DR scan (J''_L = 9.5)	Final fit (>500 lines)[a]
Rotational B''	$X\ ^2\Sigma^+$	0.0267	0.026 755 (6)
Spin-rotation γ	$X\ ^2\Sigma^+$	0.0028	0.002 505 (21)
Rotational B'	$C\ ^2\Pi$	0.0273[b]	0.026 727 (15)

[a] Reference 13.
[b] $B_{eff}(^2\Pi_{1/2}) \cong B(^2\Pi)$ since A (=750 cm^{-1}) $\gg B$.

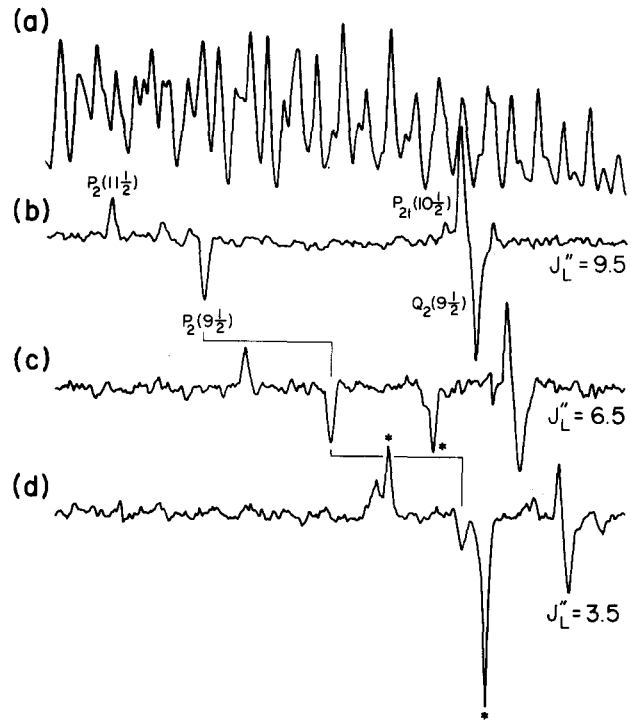

FIG. 13. Sequential DR spectra, stepping an f-parity labeled level down by increments of three. (a) pump laser spectrum (same for all DR spectra); (b) DR spectrum for J''_L = 9.5; (c) DR spectrum for J''_L = 6.5; and (d) DR spectrum for J''_L = 3.5. The lines marked by * arise from blended probe transitions.

the DR spectra is illustrated in Fig. 13, showing the case where J''_L is lowered in increments of three. The top trace [Fig. 13(a)] is the pump LIF spectrum over a portion of the region scanned in Fig. 12. In Fig. 13(b), the DR spectrum for J''_L = 9.5 is reproduced from Fig. 12(a). In the next trace, Fig. 13(c), the DR spectrum is given for J''_L = 6.5, three J's down from that in Fig. 13(b). The key to determining the relative J''_L values in Figs. 13(b) and 13(c) is to use the P_2 branch, since Fig. 13(b) establishes the line spacing in this branch. Because the (−) component of the P_2 branch in Fig. 13(c) lies at three P_2 line spacings below P_2 (−) component in Fig. 13(b), the J''_L level is three lower than that in Fig. 13(b). Similarly, the bottom trace [Fig. 13(d)] gives the DR spectrum for the case J''_L = 3.5. Note that both DR spectra for J''_L = 6.5 and 3.5 have extra features, not corresponding to those expected from the patterns in Fig. 9. These extra lines arise from accidental blends in the probe transitions resulting in two J''_L levels being monitored. These extra lines present few problems in the analysis, however, and can actually be useful as discussed below.

Once the J''_L value of one DR spectrum is established, other J''_L values for different DR spectra are readily obtained. The case where J''_L is lowered by two is particularly simple in this case since the P_2 (+) component of the lower J''_L DR spectrum will exactly coincide with the P_2 (−) feature of the higher J''_L DR spectrum. We have, in fact, used this ability to "bootstrap" J''_L to lower values in order to find the DR pattern corresponding to the branch origins of the C_2–X subband. The manner in which certain lines in the nine line pattern such as that

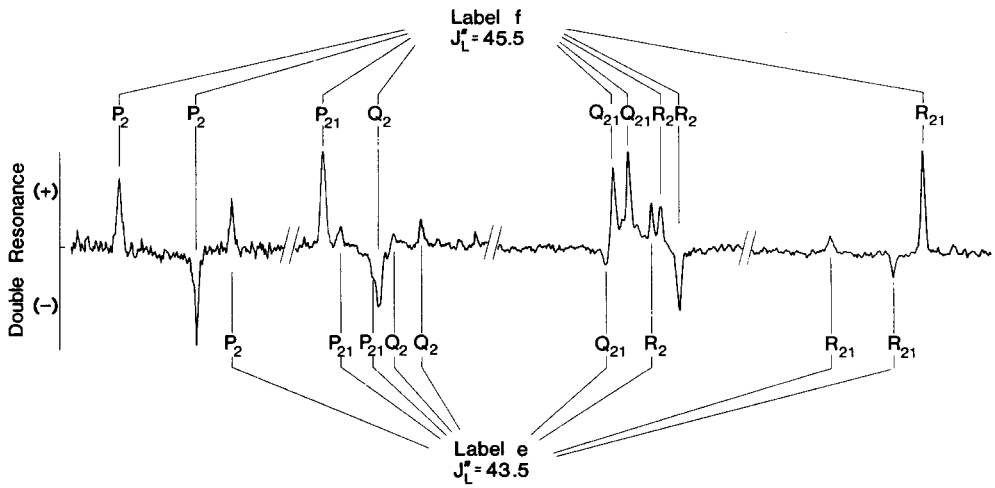

FIG. 14. Complete DR spectra illustrating behavior resulting from overlapped probe laser transitions. The strongest DR spectrum corresponds to labeling with the $Q_{12}(45.5)$ line while the weaker DR spectrum arises from the partially overlapping $P_1(43.5)$ line. These labeling transitions have opposite parity lower levels, yielding both $\gamma > 0$ phase patterns in the DR spectrum (see Fig. 9).

in Fig. 12 drop out as the $J_L'' = 1/2$ level is reached, in fact provides the first experimental determination that the spin-orbit ordering in the $C\ ^2\Pi$ state is regular, that is, $A > 0$.

We note that the choice of which subband was "probed" and which was "pumped" was based entirely on convenience. Once the assignment of the C_2–X subband was completed, it is a trivial matter to switch the roles of the lasers and assign the C_1–X subband. Now the probe laser can be placed on *known* transitions of the C_2–X subband and the C_1–X transitions can be linked to these assignments with the DR spectra.

While DR spectra such as those in Fig. 12 are readily obtained, occasionally more complex patterns are observed, as for example in Fig. 14. Here, 18 lines are found in the DR spectrum; six are (−) while the remaining 12 are (+). The nine strongest DR transitions clearly correspond to labeling an f parity level [refer to Fig. 9(a)]. It can be easily shown that this spectrum results from the f parity $J_L'' = 45.5$ labeled level. The remaining DR spectrum can be assigned using the R_{21} branch pattern. From Fig. 8, the $J_L'' = 45.5$, f parity, DR spectrum gives $R_{21}(44.5)$ as a (+) feature in the R_{21} branch. The spectrum in Fig. 14 shows two weak DR transitions to the left of the $R_{21}(44.5)$ line, with a phase pattern expected from a J_L'' of e parity [see Fig. 9(b)]. Further, the (−) R_{21} line lies one J lower in the branch than the $R_{21}(45.5)$ line, since the weak (+) and (−) lines are spaced two J's apart, defining the R_{21} branch spacing. Thus, the weak R_{21} (−) line corresponds to $R_{21}(43.5)$, revealing the labeling level for the weak DR spectrum as $J_L'' = 43.5$, e parity. The remaining "extra" DR lines in the spectrum (Fig. 14) are found to be consistent with this labeled level and all lines in the DR spectrum are accounted for. The weakness of the DR spectrum from the $J_L'' = 43.5$ (e parity) level results from the nature of the overlap between the transitions which are used to label the $J_L'' = 45.5(f)$ and $J_L'' = 43.5(e)$ levels, respectively.

Combined DR spectra, such as that in Fig. 14, are actually desirable when analyzing a spectrum. Since the phase patterns are easily separated, the DR spectra can then be recorded simultaneously for more than one J_L'' level, economizing the experimental work needed to unravel the spectrum.

We have demonstrated the use of optical–optical double resonance in analyzing congested spectra. Its power to determine absolute J numberings is illustrated by the rotational assignment of the BaI C–X system, a molecule for which no rotational information was previously available on any electronic state. This method exploits the phase information present in a single double resonance scan to establish the rotational quantum number assignment as well as to estimate both upper and lower state rotational constants. Once one double resonance scan has been obtained, it is a straightforward procedure to step through J values, requiring no guesswork. This allows one to confirm the rotational assignment, to improve the upper and lower state constants, and to establish the electronic symmetries of the states constituting the band system.

ACKNOWLEDGMENTS

The collaboration with C. R. Webster in the experimental aspects of this work and the loan of equipment from the San Francisco Laser Center are gratefully acknowledged. The selectively detected LIF spectra used in the introduction was taken with assistance from J. S. McKillop and C. Noda. RNZ also thanks the Shell Companies Foundation, Inc., for their Distinguished Chairs Program. This work is supported in part by the National Science Foundation under NSF CHE 80-06524 and by the Air Force Office of Scientific Research under AFOSR F49620-83-C-0033.

[1] W. Demtröder, *Laser Spectroscopy* (Springer, Berlin, 1981).
[2] M. Levenson, *Introduction to Nonlinear Spectroscopy* (Academic, New York, 1982), p. 66.
[3] M. A. Johnson, J. Rostas, S. Leach, and R. N. Zare, J. Chem. Phys. **80,** 2407 (1984).
[4] D. K. Hsu, D. L. Monts, and R. N. Zare, *Spectral Atlas of Nitrogen Dioxide, 5530 to 6480 Å* (Academic, New York, 1978).
[5] A. S-C. Cheung, A. M. Lyyra, A. J. Merer, and A. W. Taylor, J. Mol. Spectrosc. **102,** 224 (1983).
[6] M. Raab, G. Höning, W. Demtröder, and C. R. Vidal, J. Chem. Phys. **76,** 4370 (1982).

[7] M. A. Johnson, C. R. Webster, and R. N. Zare, J. Chem. Phys. **75,** 5575 (1981).
[8] J. B. West, R. S. Bradford, Jr., J. D. Eversole, and C. R. Jones, Rev. Sci. Instrum. **46,** 164 (1975).
[9] G. Herzberg, *Spectra of Diatomic Molecules,* 2nd ed. (Van Nostrand, New York, 1950).
[10] C. Linton, J. Mol. Spectrosc. **69,** 351 (1978).
[11] M. Dulick, P. F. Bernath, and R. W. Field, Can. J. Phys. **58,** 703 (1980).
[12] W. Demtröder, in *Case Studies in Atomic Physics,* edited by M. R. C. McDowell and E. W. McDaniel (North-Holland, Amsterdam, 1976), Vol. 6.
[13] M. A. Johnson, C. Noda, J. S. McKillop, and R. N. Zare, Can. J. Phys. **62,** 1467 (1984).
[14] M. A. Johnson, Ph.D. thesis, Stanford University, 1983.
[15] J. S. McKillop, C. Noda, M. A. Johnson, and R. N. Zare (work in progress).
[16] M. E. Kaminsky, R. T. Hawkins, F. V. Kowalski, and A. L. Schawlow, Phys. Rev. Lett. **36,** 671 (1976).
[17] W. Demtröder, D. Eisel, H. J. Foth, G. Höning, M. Raab, H. J. Vedder, and D. Zevgolis, J. Mol. Struct. **59,** 291 (1980).
[18] M. A. Johnson, J. Rostas, and R. N. Zare, Chem. Phys. Lett. **92,** 225 (1982).
[19] P. C. Cosby and H. Helm, J. Chem. Phys. **76,** 4720 (1982).
[20] J. M. Brown, J. T. Hougen, K.-P. Huber, J. W. C. Johns, I. Kopp, H. Lefebvre-Brion, A. J. Merer, D. A. Ramsay, J. Rostas, and R. N. Zare, J. Mol. Spectrosc. **55,** 500 (1975).
[21] P. J. Dagdigian, H. W. Cruse, and R. N. Zare, Chem. Phys. **15,** 249 (1976).
[22] P. J. Dagdigian, H. W. Cruse, and R. N. Zare, J. Chem. Phys. **60,** 2330 (1974).
[23] P. D. Kleinschmidt and D. L. Hildenbrand, J. Chem. Phys. **68,** 2819 (1978).
[24] M. S. Sorem and A. L. Schawlow, Opt. Commun. **5,** 148 (1972).